


# Tubulointerstitial nephritis antigen-like 1 deficiency alleviates age-dependent depressed ovulation associated with ovarian collagen deposition in mice

Masato Akaiwa<sup>1</sup> | Emiko Fukui<sup>1,2</sup> | Hiromichi Matsumoto<sup>1,2</sup> 

<sup>1</sup>Laboratory of Animal Breeding and Reproduction, Division of Animal Science, School of Agriculture, Utsunomiya University, Utsunomiya, Japan

<sup>2</sup>Center for Bioscience Research and Education, Utsunomiya University, Utsunomiya, Japan

## Correspondence

Hiromichi Matsumoto, Laboratory of Animal Breeding and Reproduction, Division of Animal Science, School of Agriculture, Utsunomiya University, Utsunomiya, Tochigi 321-8505, Japan.  
Email: matsu@cc.utsunomiya-u.ac.jp

## Funding information

JSPS KAKENHI, Grant/Award Number: 22580316, 25450390 and 18K05936

## Abstract

**Purpose:** This study aimed to examine whether the *Tinagl1* might be associated with ovulation in aged females and reproductive age-associated fibrosis in the stroma of the ovary.

**Methods:** To address the ovulatory ability and quality of ovulated oocytes, we induced ovulation by treatment with equine chorionic gonadotropin (eCG) and human chorionic gonadotropin (hCG) followed by in vitro fertilization. We also performed Picrosirius Red (PSR) staining to evaluate ovarian collagen deposition.

**Results:** As compared to ovulation in 8- to 9-month-old *Tinagl1<sup>flox/flox</sup>* mice, the number of ovulated oocytes from *Tinagl1<sup>flox/flox</sup>* mice decreased in an age-dependent manner in mice more than 10-11 months old, whereas the ovulated oocyte numbers in *Tinagl1<sup>-/-</sup>* mice decreased significantly at 14-15 months. In vitro fertilization followed by embryo culture demonstrated the normal developmental potential of *Tinagl1*-null embryos during the preimplantation period. PSR staining indicated that collagen was found throughout the ovarian stroma in an age-dependent manner in *Tinagl1<sup>flox/flox</sup>* females, whereas those distributions were delayed to 14-15 months in *Tinagl1<sup>-/-</sup>* females. This timing was consistent with the delayed timing of age-related decline of ovulation in *Tinagl1<sup>-/-</sup>* females.

**Conclusions:** The alleviation of age-associated depression of ovulation was caused by delayed ovarian collagen deposition in *Tinagl1*-null female mice.

## KEYWORDS

aging, matricellular protein, mouse, ovulation, *Tinagl1*

## 1 | INTRODUCTION

In mammals, advanced maternal physiologic age and fertility are inversely correlated.<sup>1,2</sup> Age-associated reproductive decline is multifactorial and is largely due to a constant reduction in the number of available oocytes.<sup>3-5</sup> Moreover, reduced mammalian fertility is also

influenced by oocyte quality and an oocyte's developmental potential; decreased ooplasm quality, mitochondrial defects, and abnormalities in the meiotic machinery are all potential contributors to the age-related decline in oocyte quality observed in mice and humans.<sup>1,2,6</sup> Indeed, developmental potential can be improved after transfer of oocyte genomes from aged mice into oocytes of young mice.<sup>7,8</sup>

This is an open access article under the terms of the Creative Commons Attribution License, which permits use, distribution and reproduction in any medium, provided the original work is properly cited.

© 2019 The Authors. *Reproductive Medicine and Biology* published by John Wiley & Sons Australia, Ltd on behalf of Japan Society for Reproductive Medicine.

In addition, the reduction of gamete quantity is characterized as physiologic aging. While the number of available oocytes is reduced in an age-dependent manner, rare follicles were observed in ovaries, and the ovarian cortex was almost displaced by connective tissue in aged mice.<sup>1</sup> In mice, reproductive age-associated fibrosis occurred in the stroma of the ovary, as evidenced by the observation that Picosirius Red (PSR) staining, specific for collagen I and III, was minimal in ovaries from reproductively young adult mice (6-12 weeks), increased in distinct foci in mice of mid-to-advanced reproductive age, and prominent throughout the stroma of the oldest mice in the study (>20 months).<sup>9</sup> Therefore, the distribution of extracellular matrix (ECM) components appears to be involved in age-associated reproductive decline, including ovulation.

In contrast to the ECM proteins such as collagens, which contribute to the structural integrity of the extracellular matrix by multimerization, a group of ECM proteins that do not directly play a structural role is categorized as matricellular proteins.<sup>10</sup> Matricellular proteins interact with structural matrix proteins, cell surface receptors, or extracellular factors such as growth factors and proteinases, and modulate cell-matrix interactions and cellular functions, including proliferation, differentiation, adhesion, and migration. Furthermore, several matricellular proteins that are associated with collagen deposition are known to be involved in hepatic fibrosis, including osteopontin (OPN),<sup>11-13</sup> tenascin C,<sup>14</sup> cysteine-rich acidic secreted protein (SPARC),<sup>15-17</sup> and periostin.<sup>18</sup>

Tubulointerstitial nephritis antigen-like 1 (Tinagl1, also known as adrenocortical zonation factor 1 [AZ-1] or lipocalin 7) is a matricellular protein that interacts with both structural matrix proteins and cell surface receptors.<sup>19-21</sup> Our previous study revealed that homologous mating of *Tinagl1*<sup>-/-</sup> females and *Tinagl1*<sup>-/-</sup> males showed impaired fertility during pregnancy, including failure to carry pregnancy to term and perinatal lethality.<sup>22</sup> Meanwhile, ovulation from 2- to 7-month-old *Tinagl1*<sup>-/-</sup> mice induced by equine chorionic gonadotropin (eCG) and human chorionic gonadotropin (hCG) showed that the number of ovulated oocytes did not differ compared with the number in *Tinagl1*<sup>flox/flox</sup> mice.<sup>22</sup> In vitro fertilization followed by embryo culture also demonstrated normal developmental potential of *Tinagl1*-null embryos during the preimplantation period.<sup>22</sup>

In aged mice, the ovarian cortex was almost displaced by connective tissue.<sup>1</sup> Furthermore, reproductive age-associated fibrosis was apparent in the stroma of the ovary in mice.<sup>9</sup> As *Tinagl1* is a matricellular protein, *Tinagl1* deficiency could be associated with ovulation in aged females. Our initial expectation in the present study was that age-associated depression of ovulation in aged *Tinagl1*<sup>-/-</sup> females might be slight as compared with *Tinagl1*<sup>flox/flox</sup> females. To address the ovulatory ability and quality of ovulated oocytes, we induced ovulation by treatment with eCG and hCG followed by in vitro fertilization. We also performed PSR staining in ovaries to examine the accumulation of collagen and investigated whether the amount of collagen deposition differed between *Tinagl1*<sup>-/-</sup> and *Tinagl1*<sup>flox/flox</sup> during aging.

## 2 | MATERIALS AND METHODS

### 2.1 | Animals

*Tinagl1*-deficient mice were generated as described previously.<sup>22</sup> *Tinagl1*<sup>-/-</sup> and *Tinagl1*<sup>flox/flox</sup> mice were maintained by homologous matings. These mice were in the C57BL/6NCr background. Genotype was determined by PCR analysis of genomic DNA. Mice were bred in our animal care facility. The animal experiments described here were approved by the Animal Experimentation Committee at the Utsunomiya University and were performed in accordance with the instructions in the Guide for the Care and Use of Laboratory Animals published by Utsunomiya University.

### 2.2 | Superovulation, in vitro fertilization, and embryo culture

Superovulation, in vitro fertilization, and culture of embryos were performed as previously described.<sup>22,23</sup> Female mice were subjected to superovulation by intraperitoneal injection of 5 IU eCG (ASKA Animal Health Co., Ltd.) followed by 5 IU hCG (ASKA Animal Health Co., Ltd.) 48 hours later. Ovulated oocytes from *Tinagl1*<sup>-/-</sup> or *Tinagl1*<sup>flox/flox</sup> females were then collected in human tubal fluid (HTF) medium without phenol red (HTF-P) 14 hours after hCG injection. Spermatozoa were obtained from *Tinagl1*<sup>-/-</sup> or *Tinagl1*<sup>flox/flox</sup> males and preincubated for 2-3 hours in HTF-P to allow for capacitation; the final concentration was 700 spermatozoa/ $\mu$ L. In vitro fertilization was performed with homozygous combinations of *Tinagl1*<sup>-/-</sup> or *Tinagl1*<sup>flox/flox</sup> for oocytes and spermatozoa. Four hours after insemination, the oocytes were transferred into 100  $\mu$ L of potassium simplex optimized medium (KSOM) without phenol red (KSOM-P), overlaid with paraffin liquid (Nacalai Tesque) and cultured in a humidified atmosphere with 5% CO<sub>2</sub> at 37°C.

### 2.3 | Picosirius Red (PSR) staining

Picosirius Red staining was performed as previously described<sup>9,24,25</sup> with slight modifications. Ovarian tissues were snap frozen following collection of ovulated oocytes using freezing solution (FREEZER, HOZAN) as described previously.<sup>20,21,26</sup> Frozen 10- $\mu$ m sections obtained using a cryostat were mounted onto silane-coated glass slides (Matsunami Glass Ind., Ltd.). Sections were fixed in cold acetone on ice for 10 minutes followed by washing in PBS. Slides were then immersed in a PSR staining solution prepared by dissolving Sirius Red (FUJIFILM Wako Pure Chemical Co.) in a saturated aqueous solution of picric acid (FUJIFILM Wako Pure Chemical Co.) at 0.03% w/v for 10 minutes at 23-26°C. The stained sections were then washed for 2 minutes in 0.01 N HCl, dehydrated in 100% ethanol (a total of three, 30 seconds incubations), cleared in xylene for 5 minutes, and mounted with mounting medium (Daido Sangyo Co.). ImageJ software (National Institutes of Health) was used to process color threshold images of PSR-stained ovarian tissue sections as described previously.<sup>9</sup> Three mice were used for each genotype and age group.

## 2.4 | Immunohistochemical staining of Tinagl1

Immunohistochemistry was performed as described previously.<sup>20-22</sup> Frozen 10- $\mu$ m sections from snap-frozen tissues were mounted onto silane-coated glass slides. Sections were fixed in cold acetone on ice, immersed in 3% hydrogen peroxide in methanol, and treated with 1% BSA in PBS. For the primary antibody reaction, sections were incubated with rabbit polyclonal antibody to Tinagl1. After washing, sections were incubated with biotinylated goat anti-rabbit antibody (Thermo Fisher Scientific, Inc). After incubation with horseradish peroxidase-conjugated streptavidin (Thermo Fisher Scientific, Inc), reactions were visualized using 3-amino-9-ethyl carbazole (Thermo Fisher Scientific, Inc) as a chromogen, followed by counterstaining with hematoxylin. Reddish deposits indicate the sites of immunoreaction.

## 2.5 | Statistical analysis

The relationship between age and fertility was determined by Pearson correlation coefficient and linear regression analysis. One-way factorial ANOVA followed by Fisher's protected least significant difference test was used to evaluate differences among age groups of the same genotype. Student's *t* test was used to evaluate differences between different genotypes in the same age group.  $P < .05$  was considered statistically significant.

## 3 | RESULTS

### 3.1 | Tinagl1-deficient female mice exhibit alleviation of age-related ovulation decline

*Tinagl1*<sup>flox/flox</sup> and *Tinagl1*<sup>-/-</sup> females were stimulated with hormones, and superovulated oocytes were collected. A scatterplot depicting the age (8-15 months old) and the numbers of ovulated oocytes obtained from each of the *Tinagl1*<sup>flox/flox</sup> ( $n = 46$ ) and *Tinagl1*<sup>-/-</sup> ( $n = 72$ ) females is shown in Figure 1A. The linear regression formulas for the number of ovulated oocytes ( $Y$ ) and age ( $X$ ) from *Tinagl1*<sup>flox/flox</sup>

and *Tinagl1*<sup>-/-</sup> mice were  $Y = -1.16X + 23.03$  and  $Y = -0.98X + 22.74$ , respectively. The Pearson correlation coefficients ( $r$ ) obtained from *Tinagl1*<sup>flox/flox</sup> and *Tinagl1*<sup>-/-</sup> were  $-0.64$  and  $-0.44$ , respectively, (both  $P < .05$ ). The numbers of ovulated oocytes from *Tinagl1*<sup>flox/flox</sup> mice from the different age groups are summarized in Figure 1B. The numbers of ovulated oocytes (mean  $\pm$  SEM) from 8- to 9-, 10- to 11-, 12- to 13-, and 14- to 15-month-old mice were  $12.7 \pm 0.4$  ( $n = 11$ ),  $10.3 \pm 1.0$  ( $n = 14$ ),  $8.4 \pm 1.1$  ( $n = 11$ ), and  $6.0 \pm 0.7$  ( $n = 10$ ), respectively. As compared with the 8- to 9-month-old mice, the numbers of ovulated oocytes decreased in mice more than 10-11 months old in an age-dependent manner ( $P < .05$ ). The number of ovulated oocytes from *Tinagl1*<sup>-/-</sup> mice among different age groups is summarized in Figure 1C. The number of ovulated oocytes per 8- to 9-, 10- to 11-, 12- to 13-, and 14- to 15-month-old mouse was  $12.9 \pm 1.2$  ( $n = 15$ ),  $13.7 \pm 1.2$  ( $n = 22$ ),  $10.0 \pm 0.8$  ( $n = 20$ ), and  $6.9 \pm 0.7$  ( $n = 15$ ), respectively. As compared with 8- to 9-month-old mice, the numbers of ovulated oocytes were not significantly different from those that were 10-11 and 12-13 months old; however, a significant decrease was observed by 14-15 months old ( $P < .05$ ). The number of ovulated oocytes in matched age groups from mice of different genotypes is shown in Figure 1D. In the 10- to 11-month-old group, the number of ovulated oocytes from *Tinagl1*<sup>-/-</sup> mice was higher as compared with *Tinagl1*<sup>flox/flox</sup> mice ( $P < .05$ ). These results indicate that deficiency of *Tinagl1* alleviates the age-related decline of ovulation.

### 3.2 | Cleavage of fertilized eggs is not affected by Tinagl1-deficiency

As described above, age-related declines in ovulation were alleviated in *Tinagl1*-deficient female mice. To address the developmental potential of oocytes, in vitro fertilization was employed to determine the competency of ovulated oocytes for fertilization. Cleavage of fertilized eggs to the 2-cell stage or beyond was used as a parameter for successful in vitro fertilization. The scatterplot in Figure 2A depicts the age (8-15 months old) and the percentage of cleaved eggs obtained from each of the *Tinagl1*<sup>flox/flox</sup> ( $n = 46$ ) and *Tinagl1*<sup>-/-</sup> ( $n = 72$ ) females. Linear regression formulas for the percentage of cleaved

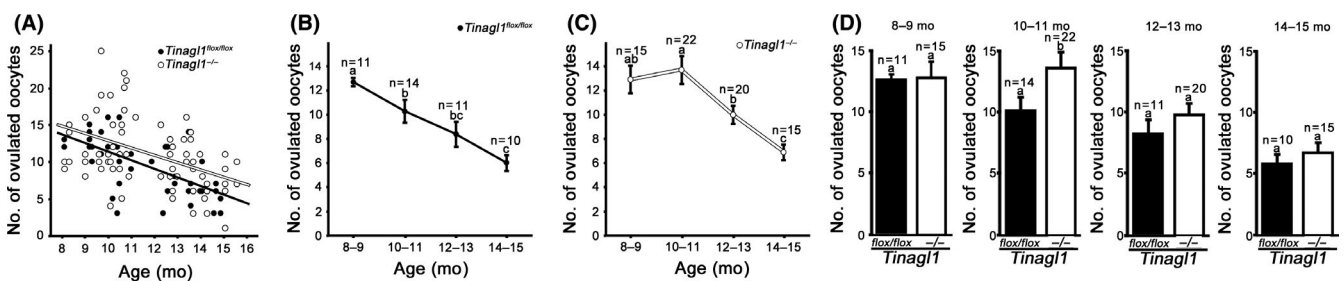


**FIGURE 1** Effect of female aging on numbers of ovulated oocytes from *Tinagl1*<sup>flox/flox</sup> and *Tinagl1*<sup>-/-</sup> mice. A, Scatterplots displaying the correlation between age and numbers of ovulated oocytes. B, Bimonthly profile of the numbers of ovulated oocytes (mean  $\pm$  SEM) derived from *Tinagl1*<sup>flox/flox</sup> females. Different letters (a-c above error bars) indicate significant differences among the age groups ( $P < .05$ ). C, Bimonthly profile of the numbers of ovulated oocytes derived from *Tinagl1*<sup>-/-</sup> females. Different letters (a-c above error bars) indicate significant differences among the age groups ( $P < .05$ ). D, Comparisons of ovulated oocyte numbers between *Tinagl1*<sup>flox/flox</sup> and *Tinagl1*<sup>-/-</sup> females in matched age groups. Different letters (a and b above error bars) indicate significant differences between *Tinagl1*<sup>flox/flox</sup> and *Tinagl1*<sup>-/-</sup> mice ( $P < .05$ )

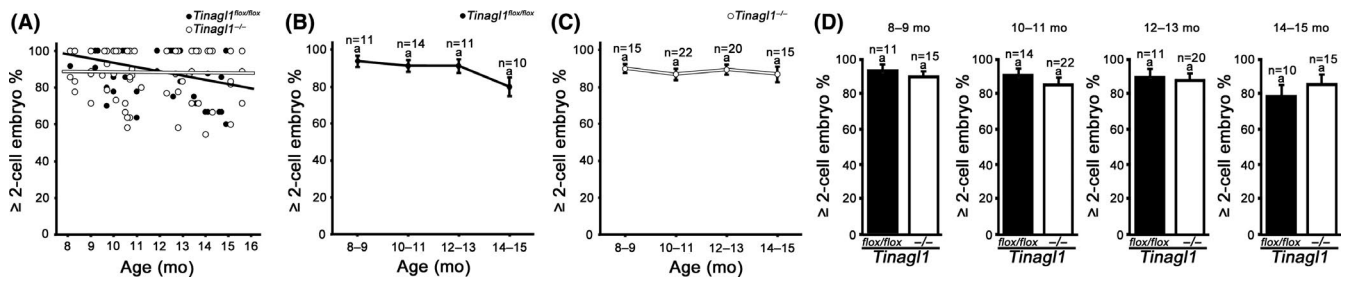


**FIGURE 2** Effect of female aging on cleavage of fertilized eggs derived from *Tinagl1<sup>flox/flox</sup>* and *Tinagl1<sup>-/-</sup>* mice to the 2-cell stage or beyond. A, Scatterplots displaying the correlation between age and percentages of fertilized eggs. B, Bimonthly profile of the percentages of fertilized eggs derived from *Tinagl1<sup>flox/flox</sup>* females. The same letter (a above error bars) indicates no significant differences among the age groups ( $P > .05$ ). C, Bimonthly profile of the percentages of fertilized eggs derived from *Tinagl1<sup>-/-</sup>* females. The same letter (a above error bars) indicates no significant differences among the age groups ( $P > .05$ ). D, Comparisons of the percentages of fertilized eggs between *Tinagl1<sup>flox/flox</sup>* and *Tinagl1<sup>-/-</sup>* mice in the same age groups. The same letter (a above error bars) indicates no significant differences between *Tinagl1<sup>flox/flox</sup>* and *Tinagl1<sup>-/-</sup>* ( $P > .05$ )

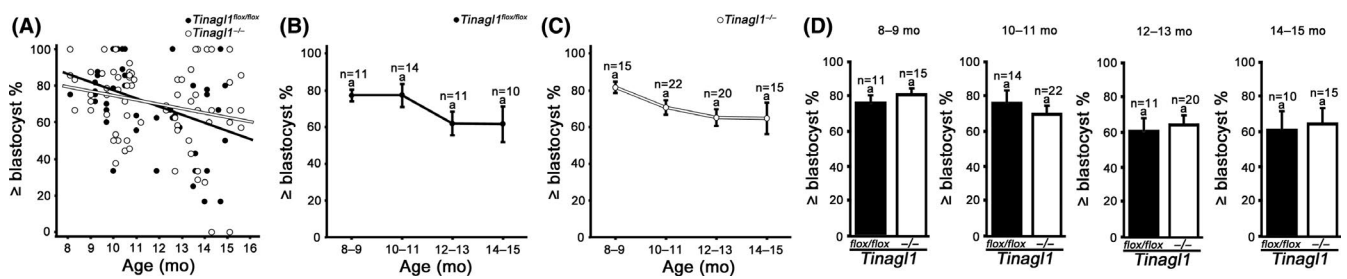


**FIGURE 3** Effect of female aging on development of oocytes derived from *Tinagl1<sup>flox/flox</sup>* and *Tinagl1<sup>-/-</sup>* females to the blastocyst stage or beyond. A, Scatterplots displaying the correlation between age and percentages of blastocysts. B, Bimonthly profile of the percentages of blastocysts derived from *Tinagl1<sup>flox/flox</sup>* females. The same letter (a above error bars) indicates no significant differences among the age groups ( $P > .05$ ). C, Bimonthly profile of the percentages of blastocysts derived from *Tinagl1<sup>-/-</sup>* females. The same letter (a above error bars) indicates no significant differences among the age groups ( $P > .05$ ). D, Comparisons of the percentages of blastocysts between *Tinagl1<sup>flox/flox</sup>* and *Tinagl1<sup>-/-</sup>* in matched age groups. The same letter (a above error bars) indicates no significant differences between *Tinagl1<sup>flox/flox</sup>* and *Tinagl1<sup>-/-</sup>* ( $P > .05$ )

eggs (Y) and age (X) obtained from *Tinagl1<sup>flox/flox</sup>* and *Tinagl1<sup>-/-</sup>* females were  $Y = -2.32X + 116.60$  and  $Y = -0.13X + 89.93$ , respectively. The Pearson correlation coefficient ( $r$ ) obtained for *Tinagl1<sup>flox/flox</sup>* was  $-0.36$  ( $P < .05$ ). In contrast, the  $r$  for *Tinagl1<sup>-/-</sup>*,  $r$  was  $-0.02$ , and there was no significant correlation between percentage of cleaved eggs and age ( $P > .05$ ). The percentages of cleaved eggs from *Tinagl1<sup>flox/flox</sup>* mice in different age groups are summarized in Figure 2B. The percentages of cleaved eggs (mean  $\pm$  SEM) from 8- to 9-, 10- to 11-, 12- to 13-, and 14- to 15-month-old mice were  $93.9 \pm 3.1$  ( $n = 11$ ),  $91.4 \pm 3.1$  ( $n = 14$ ),  $91.3 \pm 3.7$  ( $n = 11$ ), and  $80.0 \pm 5.2$  ( $n = 10$ ), respectively. There were no significant differences among these age groups ( $P > .05$ ). Figure 2C shows the percentages of cleaved eggs from *Tinagl1<sup>-/-</sup>* mice in different age groups. The percentages of cleaved eggs (mean  $\pm$  SEM) from 8- to 9-, 10- to 11-, 12- to 13-, and 14- to 15-month-old mice were  $90.2 \pm 2.5$  ( $n = 15$ ),  $86.9 \pm 3.1$  ( $n = 22$ ),  $89.5 \pm 2.8$  ( $n = 20$ ), and  $87.1 \pm 4.3$  ( $n = 15$ ), respectively. There were no significant differences among these groups ( $P > .05$ ). The percentages of cleaved eggs in matched age groups from mice of different genotypes are summarized in Figure 2D. The percentages of cleaved eggs in *Tinagl1<sup>flox/flox</sup>* and *Tinagl1<sup>-/-</sup>* mice were not significantly different for any of the age groups ( $P > .05$ ). These results indicate that

the fertilization potential of ovulated oocytes did not differ between *Tinagl1<sup>flox/flox</sup>* and *Tinagl1<sup>-/-</sup>* mice.

### 3.3 | Development to blastocyst is not affected by *Tinagl1*-deficiency

As described above, the fertilization potential of ovulated oocytes did not differ significantly between *Tinagl1<sup>flox/flox</sup>* and *Tinagl1<sup>-/-</sup>* mice. To address the further developmental ability, embryo culture was employed to determine the preimplantation development to the blastocyst stage. Development to the blastocyst stage or beyond was used as a parameter for successful in vitro development during the preimplantation period. The scatterplot in Figure 3A shows the age (8-15 months old) and the percentage of blastocysts obtained from each of the *Tinagl1<sup>flox/flox</sup>* ( $n = 46$ ) and *Tinagl1<sup>-/-</sup>* ( $n = 72$ ) genotype females. Linear regression between the percentage of blastocysts (Y) and the age (X) obtained from *Tinagl1<sup>flox/flox</sup>* and *Tinagl1<sup>-/-</sup>* mice yielded the following formulas:  $Y = -4.43X + 121.90$  and  $Y = -2.33X + 97.82$ , respectively. The Pearson correlation coefficient ( $r$ ) obtained for *Tinagl1<sup>flox/flox</sup>* females was  $-0.39$  ( $P < .05$ ). In contrast, for *Tinagl1<sup>-/-</sup>* females,  $r$  was  $-0.23$ , and there was no

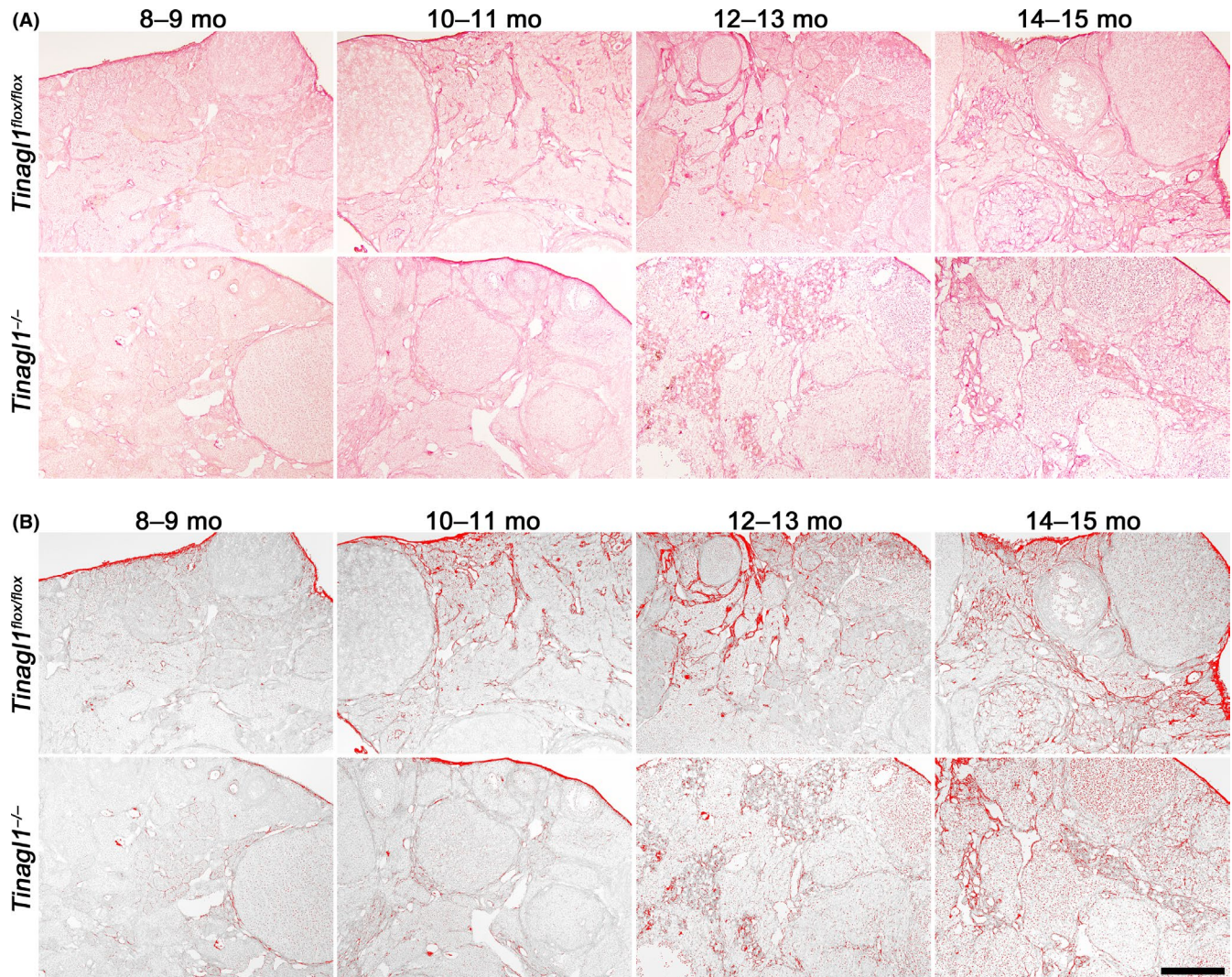


**FIGURE 4** PSR staining and the resulting processed color threshold images. PSR staining in ovaries derived from *Tinagl1<sup>flox/flox</sup>* and *Tinagl1<sup>-/-</sup>* females during aging (A). Representative processed color threshold images of PSR-stained ovarian tissue sections (B). The scale bar represents 300  $\mu$ m

significant correlation between the percentage of blastocysts and age ( $P > .05$ ). The percentages of blastocysts from *Tinagl1<sup>flox/flox</sup>* mice in different age groups are summarized in Figure 3B. The percentages (mean  $\pm$  SEM) of blastocysts from 8- to 9-, 10- to 11-, 12- to 13- and 14- to 15-months-old females were  $77.3 \pm 3.3$  ( $n = 11$ ),  $77.3 \pm 6.4$  ( $n = 14$ ),  $61.9 \pm 6.6$  ( $n = 11$ ), and  $61.6 \pm 9.8$  ( $n = 10$ ), respectively. The percentages of blastocysts were not significantly different among the age groups ( $P > .05$ ). The percentages of blastocysts from *Tinagl1<sup>-/-</sup>* mice in the different age groups are shown in Figure 3C. The percentages of blastocysts (mean  $\pm$  SEM) from 8- to 9-, 10- to 11-, 12- to 13-, and 14- to 15-month-old females were  $81.6 \pm 3.1$  ( $n = 15$ ),  $70.7 \pm 4.0$  ( $n = 22$ ),  $65.3 \pm 4.6$  ( $n = 20$ ), and  $64.8 \pm 8.6$  ( $n = 15$ ), respectively. There were no significant differences among these groups ( $P > .05$ ). Figure 3D shows the percentages of blastocysts in the same age groups from mice with different genotypes. The percentages of blastocysts did not differ significantly between *Tinagl1<sup>flox/flox</sup>* and *Tinagl1<sup>-/-</sup>* females for any of the age groups ( $P > .05$ ). These results indicate that the developmental

potential of ovulated oocytes to the blastocyst stage did not differ between the *Tinagl1<sup>flox/flox</sup>* and the *Tinagl1<sup>-/-</sup>* mice.

### 3.4 | Ovarian deposition of collagen is retarded by *Tinagl1*-deficiency

As shown in Figure 1, *Tinagl1*-deficient female mice exhibited alleviation of age-related ovulation decline. Therefore, we hypothesized that reproductive age-associated deposition of collagen may take place in the stroma of the ovary during aging and that the age-associated deposition of collagen also may be delayed in *Tinagl1<sup>-/-</sup>* as compared with *Tinagl1<sup>flox/flox</sup>* mice. To address this issue, we performed PSR staining in ovaries to examine the accumulation of collagen and investigated whether the tendency of collagen deposition differed between *Tinagl1<sup>-/-</sup>* and *Tinagl1<sup>flox/flox</sup>* mice during aging. PSR staining (Figure 4A) and the resulting processed color threshold image (Figure 4B) demonstrated intense PSR staining throughout the ovarian stroma in an age-dependent manner in *Tinagl1<sup>flox/flox</sup>* females.

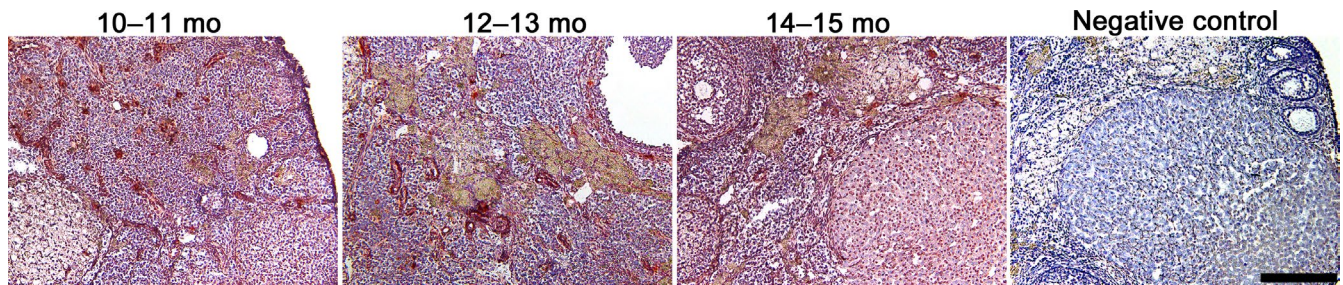


**FIGURE 5** Distribution of Tinagl1 in *Tinagl1<sup>flox/flox</sup>* mouse ovary during aging. The scale bar represents 200  $\mu$ m

Meanwhile, the appearance of intense PSR staining was delayed to 14-15 months in *Tinagl1<sup>-/-</sup>* females. This timing was consistent with the retarded timing of age-related decline of ovulation in *Tinagl1<sup>-/-</sup>* females. These results suggest that ovarian deposition of collagen is retarded by *Tinagl1* deficiency followed by alleviation of age-related ovulation decline.

### 3.5 | Distribution of Tinagl1 in ovary during aging

Immunohistochemistry was performed to determine the localization of Tinagl1 expression in *Tinagl1<sup>flox/flox</sup>* female ovary during aging. Tinagl1 protein was expressed in ovarian stroma, blood vessels, theca cells, and corpus lutea (Figure 5). In ovarian stroma, Tinagl1 expression was similar during aging.

## 4 | DISCUSSION

Previous work by our group indicated that induced ovulation in 2-7 months old *Tinagl1<sup>-/-</sup>* mice did not differ compared with *Tinagl1<sup>flox/flox</sup>* mice.<sup>22</sup> Furthermore, ovulated *Tinagl1*-null oocytes possessed developmental potential during the preimplantation period.<sup>22</sup> In contrast, our present study shows that deficiency of *Tinagl1* alleviates the age-related decline of ovulation, whereas in vitro fertilization followed by embryo culture for ovulated oocytes showed a normal developmental potential for *Tinagl1<sup>-/-</sup>* embryos during the preimplantation period as compared with *Tinagl1<sup>flox/flox</sup>* embryos.

We found that *Tinagl1*-deficient female mice exhibit alleviation of age-related ovulation decline. As compared with 8- to 9-month-old mice, the number of ovulated oocytes from *Tinagl1<sup>flox/flox</sup>* mice decreased in an age-dependent manner for females more than 10-11 months old, whereas ovulated oocyte numbers for 8- to 9-month-old *Tinagl1<sup>-/-</sup>* mice did not differ significantly from those for 10- to 11- and 12- to 13-month-old mice but decreased significantly in 14- to 15-month-old females. PSR staining intensity, indicating collagen deposition, increased in an age-dependent manner throughout the ovarian stroma in *Tinagl1<sup>flox/flox</sup>* females. Meanwhile, the observation of intense PSR-stained collagen was delayed to 14-15 months in *Tinagl1<sup>-/-</sup>* females. This timing was consistent with the retarded timing of age-related decline of ovulation in *Tinagl1<sup>-/-</sup>* females. Furthermore, Tinagl1 protein was expressed in ovarian stroma during aging. In mice, reproductive age-associated fibrosis

occurs in the stroma of the ovary. Previous study revealed that PSR staining was minimal in ovaries from reproductively young adult mice and increased in advanced reproductive age, with staining becoming prominent throughout the stroma of aged mice.<sup>9</sup> Therefore, our current findings suggest that *Tinagl1* deficiency causes delayed reproductive age-associated ovarian collagen deposition followed by an alleviation of the age-related decline of ovulation.

Fibrosis occurred in the ovarian stroma with increasing age and increased the inflammatory response in the ovary.<sup>9</sup> TINAGL1 level was increased in Fabry disease with upregulated inflammation-related pathways.<sup>27</sup> Therefore, ovarian expression Tinagl1 may be associated with inflammatory response during ovarian fibrosis. In addition, stiffness of ovary was increased with ovarian stromal fibrosis<sup>28</sup> and showed that the stiffness around the follicle was associated with follicular development.<sup>29</sup> Ovarian stromal fibrosis caused the abnormal follicular development at secondary follicle in granulosa cell-specific *Nrg1* knockout mice and resulted in decreased number of ovulated oocytes.<sup>30</sup> It has been reported that tissue stiffness and mammographic density are associated with the risk of breast carcinoma development, suggesting that matricellular proteins may influence breast carcinoma prognosis.<sup>31</sup> Moreover, Tinagl1 suppresses triple-negative breast cancer progression and metastasis.<sup>32</sup> Therefore, ovarian Tinagl1 may be associated with ovarian stiffness and depressed follicular development. Recent study reported that TINAGL1 promotes hepatocellular carcinogenesis through the activation of TGF- $\beta$  signaling mediated VEGF expression.<sup>33</sup> Because Tinagl1 is present in blood vessels,<sup>19,21,34</sup> Tinagl1 also could be related to ovarian blood vessel formation followed by constant cycles of connective tissue remodeling.

Through the processes of ovulation, the ovary undergoes constant cycles of connective tissue remodeling and wound healing, which require a complex interplay between matrix metalloproteinases (MMPs) and tissue inhibitors of metalloproteinases (TIMPs).<sup>35</sup> TIMPs inhibit the proteolytic activity of MMPs. Therefore, age-associated changes in the homeostasis of ECM may be associated with an imbalance in the activities of MMPs and TIMPs.<sup>9</sup> Furthermore, the age-associated fibrosis could be due to increased synthesis and deposition of collagen or other ECM components and/or altered post-translational modifications, because  $\alpha$ -smooth muscle actin ( $\alpha$ -SMA), which corresponds to a myofibroblast population,<sup>36,37</sup> has been observed in the ovarian stroma.<sup>9</sup> Persistent activation of myofibroblasts can cause excessive fibrotic reactions.<sup>38</sup> In addition, the

study of myofibroblast recruitment and activation in skin wounds using  $\alpha$ -SMA-GFP transgenic mice demonstrated that *Tinagl1* is linked to myofibroblast-mediated wound healing.<sup>38</sup> Therefore, it is possible that the alleviation of age-associated decline of ovulation in *Tinagl1*-deficient females is caused by reduced connective tissue remodeling during the processes of ovulation.

Under normal physiologic conditions, tissue remodeling in response to injury leads to tissue regeneration without permanent damage. Matricellular proteins are often upregulated after tissue injury<sup>39</sup> to provide extracellular matrix signals critical for tissue repair processes.<sup>40,41</sup> These non-structural ECM proteins are important during embryonic development but are typically restricted to tissue remodeling and wound repair in normal adults.<sup>42-44</sup> Indeed, several studies examining mice deficient in matricellular proteins have identified previously unsuspected consequences stemming from the lack of appropriate interactions between cells and their environment.<sup>10</sup> *Tinagl1* has been identified as a matricellular protein.<sup>19</sup> In this work, we determined that *Tinagl1* plays a role in age-associated ovulation decline caused by ovarian collagen deposition.

In conclusion, the present study describes new observations including alleviation of age-associated depression of ovulation caused by retarded ovarian collagen deposition in *Tinagl1*-null female mice. Although the numbers of ovulated oocytes from *Tinagl1*<sup>fllox/fllox</sup> mice decreased in an age-dependent manner in mice more than 10-11 months old, ovulated oocyte numbers from *Tinagl1*<sup>-/-</sup> mice did not differ significantly among 8-9, 10- to 11-, and 12- to 13-month-old females and decreased significantly by 14-15 months. However, the fertilization potential of ovulated oocytes was not significantly different between *Tinagl1*<sup>fllox/fllox</sup> and *Tinagl1*<sup>-/-</sup> mice. Furthermore, *Tinagl1* deficiency did not affect the potential of development to the blastocyst stage of ovulated oocytes during the preimplantation period as compared with *Tinagl1*<sup>fllox/fllox</sup> females. As *Tinagl1* deficiency alleviated the age-related decline of ovulation, and in vitro fertilization followed by embryo culture for ovulated oocytes showed normal developmental potential during the preimplantation period, investigation of physiologic and/or microenvironmental conditions in the ovary may further elucidate the role of *Tinagl1*. Such work could yield information that may help to improve assisted reproductive technology, although determination of the definitive role of *Tinagl1* in ovary during aging will require further studies involving the ovary-specific deletion of this gene.

## ACKNOWLEDGEMENTS

We wish to thank Eisaku Takeuchi, Saori Suzuki, Daiki Nakashima, and Akihito Takahashi (Utsunomiya University) for their expert technical assistance. This work was supported in part by JSPS KAKENHI Grant Numbers 22580316, 25450390 and 18K05936 (H.M).

## CONFLICT OF INTEREST

All authors declare no conflict of interest.

## ANIMAL STUDY

All animal experiments described here were approved by the Animal Experimentation Committee at the Utsunomiya University and were performed in accordance with the instructions in the Guide for the Care and Use of Laboratory Animals published by Utsunomiya University.

## HUMAN RIGHTS

This article does not contain any studies with human subjects performed by the any of the authors.

## ORCID

Hiroichi Matsumoto  <https://orcid.org/0000-0002-0104-6866>

## REFERENCES

1. Cui LB, Zhou XY, Zhao ZJ, Li Q, Huang XY, Sun FZ. The Kunming mouse: as a model for age-related decline in female fertility in human. *Zygote*. 2013;21:367-376.
2. Qiao J, Wang ZB, Feng HL, et al. The root of reduced fertility in aged women and possible therapeutic options: current status and future prospects. *Mol Aspects Med*. 2014;38:54-85.
3. Faddy MJ, Gosden RG, Edwards RG. Ovarian follicle dynamics in mice: a comparative study of three inbred strains and an F1 hybrid. *J Endocrinol*. 1983;96:23-33.
4. Faddy MJ, Gosden RG, Gougeon A, Richardson SJ, Nelson JF. Accelerated disappearance of ovarian follicles in mid-life: implications for forecasting menopause. *Hum Reprod*. 1992;7:1342-1346.
5. Faddy MJ. Follicle dynamics during ovarian ageing. *Mol Cell Endocrinol*. 2000;163:43-48.
6. Tarin JJ, Perez-Albala S, Cano A. Cellular and morphological traits of oocytes retrieved from aging mice after exogenous ovarian stimulation. *Biol Reprod*. 2001;65:141-150.
7. Mitsui A, Yoshizawa M, Matsumoto H, Fukui E. Improvement of embryonic development and production of offspring by transferring meiosis-II chromosomes of senescent mouse oocytes into cytoplasts of young mouse oocytes. *J Assist Reprod Genet*. 2009;26:35-39.
8. Yamada M, Egli D. Genome transfer prevents fragmentation and restores developmental potential of developmentally compromised postovulatory aged mouse oocytes. *Stem Cell Reports*. 2017;8:576-588.
9. Briley SM, Jasti S, McCracken JM, et al. Reproductive age-associated fibrosis in the stroma of the mammalian ovary. *Reproduction*. 2016;152:245-260.
10. Bornstein P, Sage EH. Matricellular proteins: extracellular modulators of cell function. *Curr Opin Cell Biol*. 2002;14:608-616.
11. Syn WK, Choi SS, Liaskou E, et al. Osteopontin is induced by hedgehog pathway activation and promotes fibrosis progression in nonalcoholic steatohepatitis. *Hepatology*. 2011;53:106-115.
12. Pritchett J, Harvey E, Athwal V, et al. Osteopontin is a novel downstream target of SOX9 with diagnostic implications for progression of liver fibrosis in humans. *Hepatology*. 2012;56:1108-1116.
13. Syn WK, Agboola KM, Swiderska M, et al. NKT-associated hedgehog and osteopontin drive fibrogenesis in non-alcoholic fatty liver disease. *Gut*. 2012;61:1323-1329.
14. El-Karef A, Yoshida T, Gabazza EC, et al. Deficiency of tenascin-C attenuates liver fibrosis in immune-mediated chronic hepatitis in mice. *J Pathol*. 2007;211:86-94.

15. Camino AM, Atorrasagasti C, Maccio D, et al. Adenovirus-mediated inhibition of SPARC attenuates liver fibrosis in rats. *J Gene Med.* 2008;10:993-1004.
16. Atorrasagasti C, Aquino JB, Hofman L, et al. SPARC downregulation attenuates the profibrogenic response of hepatic stellate cells induced by TGF- $\beta$ 1 and PDGF. *Am J Physiol Gastrointest Liver Physiol.* 2011;300:G739-G748.
17. Atorrasagasti C, Peixoto E, Aquino JB, et al. Lack of the matricellular protein SPARC (secreted protein, acidic and rich in cysteine) attenuates liver fibrogenesis in mice. *PLoS ONE.* 2013;8:e54962.
18. Huang Y, Liu W, Xiao H, et al. Matricellular protein periostin contributes to hepatic inflammation and fibrosis. *Am J Pathol.* 2015;185:786-797.
19. Li D, Mukai K, Suzuki T, et al. Adrenocortical zonation factor 1 is a novel matricellular protein promoting integrin-mediated adhesion of adrenocortical and vascular smooth muscle cells. *FEBS J.* 2007;274:2506-2522.
20. Igarashi T, Tajiri Y, Sakurai M, et al. Tubulointerstitial nephritis antigen-like 1 is expressed in extraembryonic tissues and interacts with laminin 1 in the Reichert membrane at postimplantation in the mouse. *Biol Reprod.* 2009;81:948-955.
21. Tajiri Y, Igarashi T, Li D, et al. Tubulointerstitial nephritis antigen-like 1 is expressed in the uterus and binds with integrins in decidualized endometrium during postimplantation in mice. *Biol Reprod.* 2010;82:263-270.
22. Takahashi A, Rahim A, Takeuchi M, et al. Impaired female fertility in tubulointerstitial antigen-like 1-deficient mice. *J Reprod Dev.* 2016;62:43-49.
23. Takeuchi M, Seki M, Furukawa E, et al. Improvement of implantation potential in mouse blastocysts derived from IVF by combined treatment with prolactin, epidermal growth factor and 4-hydroxyestradiol. *Mol Hum Reprod.* 2017;23:557-570.
24. Junqueira LC, Bignolas G, Brentani RR. Picrosirius staining plus polarization microscopy, a specific method for collagen detection in tissue sections. *Histochem J.* 1979;11:447-455.
25. Emde B, Heinen A, Godecke A, Bottermann K. Wheat germ agglutinin staining as a suitable method for detection and quantification of fibrosis in cardiac tissue after myocardial infarction. *Eur J Histochem.* 2014;58:2448.
26. Matsumoto H, Fukui E, Yoshizawa M, Sato E, Daikoku T. Differential expression of the motin family in the peri-implantation mouse uterus and their hormonal regulation. *J Reprod Dev.* 2012;58:649-653.
27. Ko Y, Lee C, Moon MH, Hong GR, Cheon CK, Lee JS. Unravelling the mechanism of action of enzyme replacement therapy in Fabry disease. *J Hum Genet.* 2016;61:143-149.
28. Wood CD, Vijayvergia M, Miller FH, et al. Multi-modal magnetic resonance elastography for noninvasive assessment of ovarian tissue rigidity in vivo. *Acta Biomater.* 2015;13:295-300.
29. West ER, Xu M, Woodruff TK, Shea LD. Physical properties of alginate hydrogels and their effects on in vitro follicle development. *Biomaterials.* 2007;28:4439-4448.
30. Umehara T, Kawai T, Kawashima I, et al. The acceleration of reproductive aging in Nrg1(flox/flox); Cyp19-Cre female mice. *Aging Cell.* 2017;16:1288-1299.
31. Fiorino S, Di Saverio S, Leandri P, et al. The role of matricellular proteins and tissue stiffness in breast cancer: a systematic review. *Future Oncol.* 2018;14:1601-1627.
32. Shen M, Jiang YZ, Wei Y, et al. Tinag1 suppresses triple-negative breast cancer progression and metastasis by simultaneously inhibiting integrin/FAK and EGFR signaling. *Cancer Cell.* 2019;35:64-80.e7.
33. Sun L, Dong Z, Gu H, Guo Z, Yu Z. TINAGL1 promotes hepatocellular carcinogenesis through the activation of TGF- $\beta$  signaling-mediated VEGF expression. *Cancer Manage Res.* 2019;11:767-775.
34. Wex T, Lipyansky A, Bromme NC, Wex H, Guan XQ, Bromme D. TIN-ag-RP, a novel catalytically inactive cathepsin B-related protein with EGF domains, is predominantly expressed in vascular smooth muscle cells. *Biochemistry.* 2001;40:1350-1357.
35. Curry TE Jr, Osteen KG. Cyclic changes in the matrix metalloproteinase system in the ovary and uterus. *Biol Reprod.* 2001;64:1285-1296.
36. Skalli O, Ropraz P, Trzeciak A, Benzonana G, Gillesen D, Gabbiani G. A monoclonal antibody against alpha-smooth muscle actin: a new probe for smooth muscle differentiation. *J Cell Biol.* 1986;103:2787-2796.
37. Hinz B. Myofibroblasts. *Exp Eye Res.* 2016;142:56-70.
38. Bergmeier V, Etich J, Pitzler L, et al. Identification of a myofibroblast-specific expression signature in skin wounds. *Matrix Biol.* 2018;65:59-74.
39. Tracy LE, Minasian RA, Caterson EJ. Extracellular matrix and dermal fibroblast function in the healing wound. *Adv Wound Care.* 2016;5:119-136.
40. Kyriakides TR, Maclauchlan S. The role of thrombospondins in wound healing, ischemia, and the foreign body reaction. *J Cell Commun Signal.* 2009;3:215-225.
41. Murphy-Ullrich JE, Sage EH. Revisiting the matricellular concept. *Matrix Biol.* 2014;37:1-14.
42. Bornstein P. Diversity of function is inherent in matricellular proteins: an appraisal of thrombospondin 1. *J Cell Biol.* 1995;130:503-506.
43. Ruan K, Bao S, Ouyang G. The multifaceted role of periostin in tumorigenesis. *Cell Mol Life Sci.* 2009;66:2219-2230.
44. Wu T, Ouyang G. Matricellular proteins: multifaceted extracellular regulators in tumor dormancy. *Protein Cell.* 2014;5:249-252.

**How to cite this article:** Akaiwa M, Fukui E, Matsumoto H. Tubulointerstitial nephritis antigen-like 1 deficiency alleviates age-dependent depressed ovulation associated with ovarian collagen deposition in mice. *Reprod Med Biol.* 2020;19:50-57. <https://doi.org/10.1002/rmb2.12301>